## Title
CDC7 inhibition blocks pathological TDP-43 phosphorylation and neurodegeneration



## Journal
Annals of Neurology, 74(1)

## ISSN
0364-5134

## Authors
Liachko, Nicole F
McMillan, Pamela J
Guthrie, Chris R
et al.

## Publication Date
2013-07-01

## DOI
10.1002/ana.23870

Peer reviewed

Published in final edited form as:
*Ann Neurol*. 2013 July ; 74(1): 39–52. doi:10.1002/ana.23870.

# CDC7 inhibition blocks pathological TDP-43 phosphorylation and neurodegeneration

**Nicole F. Liachko**[1,2], **Pamela J. McMillan**[3,4], **Chris R. Guthrie**[1], **Thomas D. Bird**[1,2,5], **James B. Leverenz**[3,4,5,6], and **Brian C. Kraemer**[1,2,*]

[1]Geriatric Research Education and Clinical Center, Veterans Affairs Puget Sound Health Care System, Seattle, WA 98108, USA.

[2]Department of Medicine, University of Washington, Seattle, WA 98104, USA.

[3]Mental Illness Research Education and Clinical Center, Veterans Affairs Puget Sound Health Care System, Seattle, WA 98108

[4]Department of Psychiatry and Behavioral Sciences, University of Washington, Seattle, WA 98195

[5]Department of Neurology, University of Washington, Seattle, WA 98195

[6]Parkinson's Disease Research Education and Clinical Center, Veterans Affairs Puget Sound Health Care System, Seattle, WA 98108, USA.

## Abstract

**Objective—**Kinase hyperactivity occurs in both neurodegenerative disease and cancer. Lesions containing hyperphosphorylated aggregated TDP-43 characterize amyotrophic lateral sclerosis and frontotemporal lobar degeneration with TDP-43 inclusions. Dual phosphorylation of TDP-43 at serines 409/410 drives neurotoxicity in disease models; therefore, TDP-43 specific kinases are candidate targets for intervention.

**Methods—**To find therapeutic targets for the prevention of TDP-43 phosphorylation, we assembled and screened a comprehensive RNA interference library targeting kinases in TDP-43 transgenic *C. elegans*.

**Results—**We show CDC7 robustly phosphorylates TDP-43 at pathological residues S409/410 in *C. elegans, in vitro,* and in human cell culture. In FTLD-TDP cases, CDC7 immunostaining overlaps with the phospho-TDP-43 pathology found in frontal cortex. Furthermore PHA767491, a small molecule inhibitor of CDC7, reduces TDP-43 phosphorylation and prevents TDP-43 dependent neurodegeneration in TDP-43 transgenic animals.

**Interpretation—**Taken together these data support CDC7 as a novel therapeutic target for TDP-43 proteinopathies including FTLD-TDP and ALS.

[*]To whom correspondence should be addressed at: Veterans Affairs Puget Sound Health Care System S182 1660 South Columbian Way Seattle, WA 98108 Phone (206) 277-3275 Fax (206) 764-2569 kraemerb@u.washington.edu.

**Author contributions** N.L., T.B., and B.K conceived and designed the experiments. N.L. performed *C. elegans* and cell culture experiments. P.M. performed human immunohistochemistry. C.G. performed cell culture experiments. N.L., P.M., J.L., and B.K. analyzed data. N.L., P.M., and B.K. wrote the paper.

**Competing financial interests** The authors declare no competing financial interests.

**Keywords**

amyotrophic lateral sclerosis (ALS); frontotemporal lobar degeneration (FTLD); TDP-43; *Tardbp*; neurodegeneration; neurotoxicity; neuroprotection; CDC7; TTBK1; TTBK2; kinase; phosphorylation; PHA767491

## INTRODUCTION

Pathological dysregulation of kinase activity occurs in a variety of different human diseases including most cancers and neurodegenerative disorders. Consequently, diverse kinases implicated in cell viability or replication have been the subject of kinase inhibitor development campaigns for the treatment of human cancers[1] with over a dozen FDA approved compounds for various cancers in the clinic. At present no kinase inhibitors have been approved by the FDA for neurodegenerative disease despite clear evidence of similar aberrant kinase activation in both type of disorders [2]. Here we describe a kinome wide screen for kinases involved in TDP-43 mediated neurodegeneration and supply evidence for the possible repurposing of PHA767491, a kinase inhibitor developed as an anticancer compound, for use in preventing neurodegeneration caused by TDP-43 proteinopathy.

Proteinaceous aggregates are a ubiquitous feature of neurodegenerative diseases. Aggregates containing ubiquitinated, hyperphosphorylated TDP-43 protein characterize nearly all cases of amyotrophic lateral sclerosis (ALS) and most frontotemporal lobar degeneration (FTLD-TDP) cases [3, 4]; mutations in TDP-43 cause heritable forms of ALS {reviewed in [5]}. ALS is a progressive neurodegenerative disease distinguished by loss of motor neurons, muscle wasting and deterioration of motor control, and early death [6]. FTLD is a major cause of mid to late life dementia and displays loss of neurons in the frontal and temporal lobes of the brain, major behavioral and cognitive changes, and shortened lifespan [7]. Recent studies have highlighted an overlapping spectrum of disease with TDP-43 pathology and features of both ALS and FTLD driven by hexanucleotide repeat expansion within C9ORF72 [8, 9]. Furthermore, TDP-43 positive aggregates have been identified in a growing number of other neurodegenerative diseases, including Alzheimer's disease, hippocampal sclerosis, dementia with Lewy bodies, Pick's disease, argyrophilic grain disease, and corticobasal degeneration [10, 11]. Pathological TDP-43 is hyperphosphorylated at discrete sites on the protein, mostly clustered in the C-terminus of the protein [12]. Serines 409 and 410 (S409/410) are the most robust and consistent sites of pathological phosphorylation in the TDP-43 C-terminus [13, 14]. Antibodies against phosphorylated S409/410 recognize abnormal inclusions in ALS and FTLD-TDP, and are used as a diagnostic tool to confirm TDP-43 proteinopathy in human disease. We previously demonstrated that phosphorylation at S409/410 drives neurotoxicity in a *C. elegans* model of TDP-43 proteinopathy [15]. Small molecule inhibition of the kinase or kinases responsible for TDP-43 phosphorylation may be a novel neuroprotective approach for intervention in ALS and FTLD-TDP. However, disease relevant kinase targets have not been identified *in vivo*. Recombinant casein kinase-1 (CK1) has been shown to phosphorylate TDP-43 at multiple sites including S409/410 *in vitro* [16] and CK1 inhibitors reduce but do not eliminate TDP-43 phosphorylation in mammalian cell culture [17]. Thus, other kinases besides CK1 contribute to pathological TDP-43 phosphorylation. To this end, we have screened over 450 *C. elegans* kinases by RNAi to identify target kinases that affect TDP-43 driven behavioral phenotypes. We have identified one kinase, CDC-7, responsible for pathological TDP-43 phosphorylation in transgenic *C. elegans* and human cells. Small molecule inhibition of CDC-7 by PHA767491 robustly reduces TDP-43 phosphorylation and prevents TDP-43 dependent neurodegeneration.

## RESULTS

Tandem phosphorylation at TDP-43 serines 409 and 410 (pS409/410) is a consistent and robust marker of TDP-43 pathology in ALS and FTLD-TDP [13, 14]. Our previous work in TDP-43 transgenic *C. elegans* demonstrated a causal relationship between neurodegeneration and S409/410 phosphorylation of familial ALS mutated versions of TDP-43. To identify potential kinase inhibitor targets for ALS and FTLD-TDP therapeutics, we undertook a comprehensive RNAi screen of *C. elegans* kinases to determine which kinases are responsible for TDP-43 phosphorylation. We assembled an RNAi library targeting 453 predicted kinases and kinase-like genes in *C. elegans* (95% coverage of the predicted kinases found in the *C. elegans* genome), and tested it in transgenic *C. elegans* expressing ALS-mutant M337V TDP-43 (M337V) (Supplementary Table 1). M337V animals have severe movement defects, including coiling, uncoordinated locomotion, and paralysis [15]. Therefore, we screened animals treated with RNAi targeting each kinase for improvement in the motor phenotype of M337V. The library was screened in its entirety twice. Potential TDP-43 kinases selected from the screen suppressed the movement defects of M337V to an extent equivalent to animals treated with RNAi targeting TDP-43 itself. The identity of positive RNAi clones was confirmed by direct DNA sequencing, and then tested for behavioral effects in the absence of TDP-43 to ensure movement phenotypes are not the result of a hyper-motile phenotype. Candidate kinases with human homologs that act on serine and/or threonine residues (S/T) were selected for further analysis. A total of 12 candidate S/T kinases were identified that improved M337V behavior following RNAi treatment (Table 1).

### *cdc-7* and C55B7.10 kinase null mutants improve M337V behavior and reduce TDP-43 phosphorylation

To confirm the potential neuroprotective effect observed by RNAi against specific kinases, we generated TDP-43 transgenic animals with deletion mutants eliminating the kinase active domain of the gene of interest (Table 1). While most of the kinase mutants did not visibly improve TDP-43 behavioral phenotypes, two of the TDP-43 kinase mutants have partially restored motor function as indicated by more coordinated, natural, and rapid movement than the parental TDP-43 transgenic strain. To quantify these observations, we measured the number of spontaneous head movements and the number of body movements of individual animals. *cdc-7*(−/−);M337V and C55B7.10(−/−);M337V demonstrated significantly more movements than M337V alone (Fig. 1a, b). The extent of restored locomotion was also measured by radial locomotion assay (Fig. 1c). C55B7.10(−/−)significantly improved TDP-43 movement defects in this assay, while *cdc-7*(−/−) did not. However, when we tested the *cdc-7*(−/−) mutant in the absence of the M337V transgene, we noticed that while it had grossly normal body position and movement, the animals were profoundly lethargic (Supplementary Fig. 1), which may confound efforts to measure motor improvements in M337V animals.

It is possible CDC7 and C55B7.10 modulate TDP-43 toxicity by controlling TDP-43 phosphorylation. To test this, we measured TDP-43 phosphorylation in the kinase mutant animals by immunoblotting with pS409/410 TDP-43 specific antibodies. We observed that C55B7.10(−/−) and *cdc-7*(−/−) robustly decreased TDP-43 phosphorylation (Fig. 2a, b). Total levels of TDP-43 were also apparently reduced, although this reduction was not significantly different from M337V alone (Fig. 2c). Thus, kinase loss of function decreases pS409/410 TDP-43 as well as improving motor function and restoring normal lifespan.

The data suggests C55B7.10 and *cdc-7* are *C. elegans* kinases acting directly or indirectly to promote the phosphorylation of transgenically expressed human TDP-43 in neurons. The human homologs of these genes are thus candidate TDP-43 kinases acting to phosphorylate

pathological TDP-43 in ALS and FTLD-TDP. To identify the mammalian homologs of C55B7.10 and *cdc-7*, we employed an NCBI BLAST search to compare the *C. elegans* kinase domain protein sequences against the database of human proteins, and the reciprocal BLAST results comparing the human protein kinase domain against the database of *C. elegans* proteins (Supplementary Table 2). C55B7.10 has identity to the tau tubulin kinases TTBK1 and TTBK2, which are implicated in the pathological phosphorylation of tau in animal models [18, 19], Alzheimer's disease [20, 21], and SCA11 [22] (Table 1). *cdc-7* is the only *C. elegans* homolog of the cell division cycle kinase 7 (CDC7)[23], which has multiple roles including promoting initiation and maintenance of DNA replication [24], chromosome segregation during meiosis and mitosis [25, 26], and DNA damage checkpoint response [27] (Table 1).

## CDC7 but not TTBK1/2 directly phosphorylates TDP-43 and modulates TDP-43 toxicity *in vivo*

CDC7, TTBK1, and TTBK2 may directly phosphorylate TDP-43 at S409/410, or they may act indirectly to promote TDP-43 phosphorylation by activating another kinase or kinase cascade targeting TDP-43. To test whether these kinases directly phosphorylate TDP-43, we incubated purified active human CDC7, TTBK1, or TTBK2 with purified recombinant GST-tagged full-length TDP-43, and examined phosphorylation at S409/410 by immunoblot. We found that CDC7 in complex with its kinase co-activator DBF4 phosphorylated both wild-type and fALS mutant M337V GST-TDP-43 fusion proteins (Fig. 2d). In contrast, neither TTBK1 nor TTBK2 phosphorylated TDP-43 under any conditions tested, indicating these kinases may not directly phosphorylate TDP-43 but instead may be acting upstream of CDC7 or other direct TDP-43 kinases not yet identified. Likewise, the combined incubation of TTBK1/2 with TDP-43 failed to yield any detectable pS409/410 TDP-43 (Fig. 2d). These data demonstrate that mammalian CDC7 directly phosphorylates TDP-43, indicating it is a primary TDP-43 kinase. Due to its direct effect on TDP-43 phosphorylation, the remainder of this study focuses on the relationship between CDC7 and TDP-43 phosphorylation.

It is possible an increase in CDC7 protein drives TDP-43 phosphorylation. Glutathione depletion by treatment with ethacrynic acid (EA) induces robust TDP-43 phosphorylation [17]. We examine CDC7 protein levels in HEK 293 cells following treatment with EA, and we observe a moderate increase in CDC7 levels and a robust increase in phosphorylated TDP-43 (Fig. 2e). To test whether increased levels of CDC7 are sufficient to promote TDP-43 phosphorylation *in vivo*, we generated transgenic *C. elegans* that overexpress *cdc-7* (*cdc-7* o/ex). The *cdc-7* o/ex animals appeared grossly normal in morphology, movement, growth, and reproduction. However, animals carrying both *cdc-7* and any TDP-43 transgene were profoundly affected. Double transgenic animals generated by crossing *cdc-7* o/ex with M337V appeared at rates much lower than expected. The few surviving *cdc-7* o/ex;M337V animals were paralyzed, extremely slow growing or developmentally arrested, and had very few or no viable offspring. We compared the number of *cdc-7* o/ex;M337V animals observed to the number expected based on normal Mendelian segregation, and found greater than 80% synthetic lethality for this genotype (Fig. 3a and Supplementary Table 3). This effect was observed with three different *cdc-7* o/ex lines generated (Supplementary Table 3). *cdc-7* o/ex had less than 10% synthetic lethality in animals expressing GFP alone (Supplementary Table 3), indicating its toxicity is not due simply to the presence of an additional transgene or additional motor neuron protein load alone. To test whether *cdc-7* o/ex toxicity is specific for the M337V TDP-43 mutation or transgene, we generated *cdc-7* o/ex transgenic animals with fALS TDP-43 mutations G290A and A315T, respectively, and saw comparable or worse synthetic lethality to that observed with M337V (Supplementary Table 3), indicating this is not a transgene or mutation specific effect.

Wild-type TDP-43 expressed in *C. elegans* has a moderate motor dysfunction phenotype, little if any detectable pS409/410 TDP-43, and no degeneration of GABA motor neurons [15]. To test whether wild-type TDP-43 is sensitive to *cdc-7* o/ex, we repeated our synthetic lethality analysis for *cdc-7* o/ex;WT TDP-43 animals. We observed more than 50% lethality of *cdc-7* o/ex;WT TDP-43 (Fig. 3a, Supplementary Table 3). In addition, surviving *cdc-7* o/ex;WT TDP-43 animals were paralyzed, slow growing, and relatively infertile, indicative of robust enhancement of the toxicity of wild-type TDP-43.

To clarify whether phosphorylation at S409/410 is important for the synthetic lethality of *cdc-7* o/ex and TDP-43, we crossed *cdc-7* o/ex animals to phosphorylation null mutant TDP-43 with substitutions of serines 409 and 410 for alanine (*cdc-7* o/ex;M337V-AA) [15]. Progeny from these animals had significantly lower lethality compared to WT or M337V TDP-43, and *cdc-7* o/ex;M337V-AA animals had movement and growth comparable to the TDP-43 transgene alone. (Fig. 3a, Supplementary Table 3). Thus, CDC-7 mediated enhancement of TDP-43 toxicity requires pS409/410 phosphorylation, suggesting the synthetic lethality and enhanced behavioral phenotypes observed with *cdc-7* o/ex are due to an increase in CDC7 driven TDP-43 phosphorylation.

To determine whether TDP-43 phosphorylation increases in *cdc-7* o/ex transgenic animals, we collected animals from the rare class of double homozygous *cdc*-7 o/ex;TDP-43 transgenics and measured phosphorylation levels by immunoblot with a S409/410 phosphorylation specific antibody. We observed an increase in phosphorylation of both wild-type TDP-43 and mutant TDP-43, respectively (Fig. 3b). Interestingly, we also observed an increase in the amount of total full length 45kDa and truncated 35kDa TDP-43 in both wild-type and mutant TDP-43 animals. The increase in TDP-43 levels is particularly striking in wild-type TDP-43 transgenic animals, which normally have a very low level of detectable TDP-43 (see Fig. 3b overexposure). This may indicate phosphorylation is stabilizing TDP-43 and preventing normal protein turnover.

Animals expressing mutant TDP-43 exhibit age-dependent neurodegeneration of GABAergic motor neurons [15]. To test whether overexpression of *cdc-7* promotes neurodegeneration, we constructed M337V;*cdc-7* o/ex animals with GABAergic motor neurons marked by GFP. We observed earlier neuronal death in these animals compared with M337V alone (Fig. 3c). *cdc-7* o/ex alone had no detrimental effect on the GABAergic neurons.

Wild-type TDP-43 exhibits little or no age-dependent degeneration of its GABAergic motor neurons [15]. To test whether *cdc-7* overexpression would potentiate neurodegeneration in WT TDP-43 transgenic *C. elegans*, we generated WT TDP-43;*cdc-7* o/ex animals with GFP labeled GABAergic motor neurons. These animals displayed a dramatic increase in neurodegeneration, consistent with their exacerbated behavioral impairments (Fig. 3d, e, f).

Since phosphorylation by CDC-7 promotes TDP-43 toxicity and neurodegeneration in *C. elegans*, we tested whether the *cdc-7*(−/−) kinase null mutant will protect against neurodegeneration in M337V animals. We observed that *cdc-7(−/−);*M337V animals had significantly fewer lost neurons, indicating that preventing CDC7 kinase activity is protective against TDP-43 neurotoxicity (Fig. 3g).

## CDC7 and phosphorylated TDP-43 are co-expressed in FLTD-TDP frontal cortex neurons

If CDC7 is involved in the pathological phosphorylation of TDP-43 it should be expressed in the human brain in regions where TDP-43 lesions occur. Immunohistochemistry for CDC7 and phosphorylated TDP-43 was performed on frontal cortex sections from 6 FTLD cases and 6 normal control cases to determine if there was overlap in the expression of this

kinase and its purported target. Of the FTLD cases tested, 5 were of unknown genetic etiology, while 1 case had a causative mutation in progranulin [28, 29]. Figure 4 demonstrates that CDC7 immunoreactivity is present in pyramidal neurons in the frontal cortex of both normal and FTLD cases. There were no obvious differences in CDC7 immunoreactivity observed in progranulin mutant FTLD versus sporadic FTLD. Immunoreactivity appears to be more prominent in the deeper cortical layers and a cytoplasmic sub-cellular localization predominates. In FTLD cases, lesions containing phosphorylated TDP-43 are also prominent in the deeper layers of the cortex, as well as cortical layer 2 (Fig. 4c), regions well known to display this pathology [3, 4]. We performed double label immunohistochemistry to determine if CDC7 and phospho TDP-43 co-localized within the same cell. We observed a subset of cortical neurons were immunoreactive for both proteins, while other neurons were only immunoreactive for CDC7 or phospho TDP-43 (Fig. 4d, e).

### PHA767491 decreases TDP-43 phosphorylation *in vitro* and *in vivo*

The genetic experiments described above suggest inhibiting CDC7 kinase activity reduces phosphorylation of TDP-43 and the consequent neurodegeneration. To test whether small molecule CDC7 inhibitors block phosphorylation of TDP-43 *in vitro*, we incubated purified CDC7 and TDP-43 with increasing concentrations of the CDC7 ATP-competitive inhibitor PHA767491 [30, 31]. We examined levels of pS409/410 TDP-43 by immunoblot, and observed complete inhibition of TDP-43 phosphorylation with 125μM PHA767491 treatment (Fig. 5a). This is approximately 100 fold molar excess of drug relative to kinase (CDC7), 10 fold excess relative to substrate (TDP-43), and 2 fold excess relative to ATP.

To determine whether PHA767491 will prevent TDP-43 phosphorylation in intact cells, we incubated motor neuron enriched NSC-34 cells with PHA767491, and then treated the cells with EA to induce phosphorylation of endogenous TDP-43. We observed that most TDP-43 phosphorylation was prevented by treatment with 10μM PHA767491 (Fig. 5b). To test whether inhibition of CDC7 in the context of a whole organism would be effective at preventing TDP-43 phosphorylation, we assayed *C. elegans* raised on plates containing increasing concentrations of PHA767491. We observed severe growth retardation at concentrations beyond 90μM, consistent with PHA767491 affecting CDC7's known role as a cell cycle promoting kinase. When we measured treated animals for changes in TDP-43 phosphorylation by immunoblot, we observed a significant decrease in the level of TDP-43 phosphorylation at 70μM PHA767491, a concentration of inhibitor that had mild effects on *C. elegans* growth (Fig. 5c, d).

For small molecule inhibition of the TDP-43 kinase CDC7 to be a viable treatment for TDP-43 proteinopathies such as FTLD-TDP and ALS, it should prevent not only phosphorylation of TDP-43 but the consequent neurodegeneration *in vivo*. To test this, we raised M337V TDP-43 transgenic *C. elegans* in the presence of 70μM PHA767491 and scored for loss of GABAergic motor neurons. We observed significantly fewer lost neurons in animals treated with PHA767491 relative to controls (Fig. 5e).

## DISCUSSION

Phosphorylation of aggregated TDP-43 at S409/410 is a defining hallmark of TDP-43 proteinopathies including ALS and FTLD-TDP [13, 14]. Elucidating the mechanisms controlling phosphorylation of TDP-43 is important for an understanding of the biology of TDP-43 proteinopathies, as well as a critical step toward developing therapeutics. To identify relevant targets for small molecule inhibition, we interrogated the kinome by RNAi in a *C. elegans* model of TDP-43 proteinopathy for effects on TDP-43-driven behavioral phenotypes. *C. elegans* is a good model system in which to conduct such a screen because it has representative homologs for over 80% of human kinase families, and exhibits a robust

RNAi response suitable for high-throughput RNAi screening [32, 33]. Indeed such *C. elegans* based RNAi screens have provided valuable insights into neurodegeneration mechanisms [34-36]. Using a similar approach, we identified twelve kinases that improve TDP-43 model animals' movement defects by gene specific RNAi. Follow-up validation of RNAi hits with genetic null mutations yielded two kinase mutants, *cdc-7*(−/−) and C55B7.10 (−/−) that significantly improved TDP-43 behavioral phenotypes and reduced phosphorylation of TDP-43 at S409/410.

We examined the ability of the human homologs of these kinases, CDC7, TTBK1 and TTBK2, to phosphorylate TDP-43 *in vitro*. Interestingly, only CDC7 was able to directly phosphorylate TDP-43 in an *in vitro* kinase assay. While we cannot rule out the possibility of sub-optimal *in vitro* kinase assay conditions of TTBK1/2 for TDP-43, these conditions are adequate for limited tau phosphorylation *in vitro*. Thus, it seems more likely that TTBK1 and TTBK2 do not directly phosphorylate TDP-43, but rather act upstream to regulate additional TDP-43 kinases. Developing and testing inhibitors for the kinases controlling TDP-43 phosphorylation through CDC7 and potentially other direct kinases will be important future work.

EA treatment causes concomitant induction of CDC7 expression and TDP-43 phosphorylation in mammalian cells, arguing for a direct, biologically relevant link between the two. In addition, increased levels of CDC-7 robustly worsen the phenotypes of the *C. elegans* model of TDP-43, with high levels of lethality. Surviving animals display much more severe TDP-43 phenotypes including paralysis, developmental arrest, infertility, neurodegeneration, and increased TDP-43 phosphorylation. Taken together, CDC7 is a direct TDP-43 kinase that regulates pathological TDP-43 phosphorylation in cellular and animal models of TDP-43 proteinopathy. Selective inhibition of TDP-43 phosphorylation holds promise as a therapeutic strategy for TDP-43 proteinopathies such as FTLD-TDP and ALS. As a proof of concept, we demonstrate PHA767491, an ATP competitive inhibitor of the kinase CDC7, prevents TDP-43 phosphorylation *in vitro* and *in vivo*. Furthermore, PHA767491 treatment prevents neurodegeneration in intact TDP-43 transgenic animals.

The findings from the FTLD-TDP patient immunohistochemistry studies support a role for CDC7 in the regulation of pathological TDP-43 phosphorylation in human TDP-43 proteinopathy diseases. We demonstrate CDC7 immunoreactivity in FTLD-TDP cases in the frontal cortex, a brain region known to exhibit high levels of pS409/410 TDP-43 pathology. Additionally, we found many cells that were co-labeled with both CDC7 and phosphorylated TDP-43. We observed similar staining in both sporadic FTLD-TDP and progranulin mutation carriers. Interestingly, CDC7 was predominantly cytoplasmic in neurons, a result somewhat surprising given that CDC7 is a nuclear protein in normal dividing cells [37, 38]. CDC7 protein contains nuclear localization, retention, and export signals, which provide a mechanism for regulated movement between the nucleus and cytoplasm [37], and it has been shown to be actively imported into the nucleus during G1 phase of the cell cycle [38]. It is not known what functions CDC7 may have in the cytoplasm or in post-mitotic cells like neurons. However, CDC7's surprising presence in neuronal cytoplasm places it in the same cellular compartment as pathological TDP-43. Of note, normal control patients also exhibited neuronal cytoplasmic CDC7, suggesting as yet unknown functions for this kinase in normal post-mitotic neurons. While many cells co-expressed the two proteins, other cells were only immunoreactive for CDC7 or phosphorylated TDP-43. Those immunoreactive for CDC7 alone are similar to control neurons, and may indicate neurons unaffected by pathological TDP-43 or neurons at an earlier stage of pathology in which phosphorylated TDP-43 has not yet accumulated to detectable levels. In contrast, neurons immunoreactive for phosphorylated TDP-43 but not CDC7 may represent a later stage in the disease course

where CDC7 becomes down-regulated as the cell succumbs to the accumulation of high levels of toxic pS409/410 TDP-43, culminating in cell death.

CDC7 has been studied extensively for its roles in DNA replication and DNA damage response [39]. While CDC7's studied role in DNA synthesis represents a relatively brief period in the life of a cell, CDC7 protein levels remain constant after cell division, arguing for additional functions for this kinase unrelated to DNA replication. The kinase activator DBF4 is required for cell cycle related functions of CDC7, and our data has shown that *in vitro*, the kinase activator DBF4 is sufficient to allow CDC7 phosphorylation at the pathological S409/410 residues of TDP-43. However, as DBF4 protein levels drop dramatically following S-phase [40-42], it is possible that unidentified CDC7 kinase activators act in conjunction with CDC7 to promote TDP-43 phosphorylation *in vivo*. Neurons have exited the cell cycle and exist as mitotically quiescent cells, and it is not clear what role a cell cycle protein like CDC7 might have at this stage. Clarifying the role of neuronal CDC7 in pathological TDP-43 phosphorylation will be a critical area of future research.

Our data indicate that phosphorylation of TDP-43 at serines 409 and 410 is a key modification that promotes TDP-43 toxicity *in vivo*. Increased phosphorylation of wild type or mutant TDP-43 driven by CDC-7 overexpression is highly neurotoxic, while decreased phosphorylation is neuroprotective. There are several possibilities for how TDP-43 phosphorylation contributes to disease. Phosphorylation may alter TDP-43 interactions with target mRNAs or co-factors important for normal TDP-43 function. It may change protein localization, driving TDP-43 from the nucleus to the cytoplasm or promote TDP-43 aggregation. Our data indicate that phosphorylation may stabilize TDP-43 and prevent or delay protein turnover, consistent with previously published data [12, 43-45]. Cellular homeostasis requires consistent TDP-43 protein levels , with negative consequences for too little or too much protein [46]. Phosphorylation may both reduce the amount of functional RNA bound TDP-43 and increase the amount of free aggregation prone TDP-43, producing a potentially toxic cellular environment.

We have demonstrated that TDP-43 phosphorylation is regulated by a small number of kinases. Among these, CDC7 directly phosphorylates TDP-43 on serines 409 and 410 both *in vitro* and *in vivo*. Furthermore, inhibition of CDC7 activity with PHA767491 at levels permissive of cell division and growth *in vivo* is sufficient to reduce TDP-43 phosphorylation and prevent neurodegeneration. Thus, CDC7 appears to be a suitable target kinase for therapeutic interventions in patients with primary TDP-43 proteinopathies such as ALS and FTLD-TDP. Several independent CDC7 focused inhibitor screening campaigns have been completed yielding distinct structural classes of CDC7 specific inhibitors, which are under further development as potential cancer treatments [30, 47-51] . Testing known CDC7 inhibitors on mammalian animal models exhibiting authentic disease-like pS409/410 positive TDP-43 pathology will be an important next step. Because CDC7 has critical roles in the cell cycle, identifying an inhibitor capable of ameliorating CDC7 phosphorylation of TDP-43 without completely disrupting other essential CDC7 mitotic functions could lead to viable long-term treatment for patients suffering from TDP-43 proteinopathies. Excitingly, recent studies have shown reduction of pathological TDP-43 could potentially allow recovery of motor functions even after deposition of abnormal TDP-43 and onset of motor dysfunction [52].

# METHODS

## Transgenics and Strains

For a complete list of strains and transgenic *C. elegans* used, please see Supplemental Methods. Strains were maintained at 16°C. Experiments involving *C. elegans* were performed at room temperature unless otherwise noted.

## RNAi screening

The list of predicted kinase genes in *C. elegans* was derived from the *C. elegans* kinome project [53]. The RNAi library targeting *C. elegans* kinases (453 genes, about 95% coverage) was picked from the Ahringer [54] and Vidal [55] genome-wide RNAi libraries into 96-well plates and stored as frozen bacterial stocks. Testing individual RNAi constructs by feeding RNAi was performed essentially as described [54]. Testing was done in an *eri-1(−/−);lin-15*(−/−) RNAi enhancing mutant background [56]. Staged embryos were plated, grown at 16°C for 8-9 days, and then a mixed population of 1st generation gravid adults with 2nd generation L2-L3 animals were scored semi-quantitatively for suppression or enhancement of movement defects. Each RNAi construct was tested on duplicate populations, and each population was scored blind on two successive days, resulting in 4 observations per treatment. The entire library was screened in this manner twice, resulting in 8 total observations for each RNAi treatment. RNAi treated animals that showed movement comparable or better than animals treated with TDP-43 RNAi on multiple observations were selected as candidates of interest. Positives candidates were confirmed by sequencing the RNAi plasmid, followed by retesting at least twice in a low-throughput capacity on TDP-43 transgenic animals, and testing in an *eri-1(−/−);lin-15(-)* background alone for the absence of hypermotile phenotypes.

## Movement assays

Un-stimulated behavior of synchronized day 1 adult animals grown at 25°C was recorded on a Hamamatsu C5810 video camera. 30 second movies of individuals were analyzed for head movements to the left or right of the central body axis (lateral head movement) and for attempts at forward motion (forward advancement). Animals in extensive contact with neighbors and individuals with indistinct head movements as recorded were eliminated from analysis. Radial locomotion assays were employed as described [15]. Statistical analysis was performed using GraphPad Prism software.

## Immunoblotting

Equivalent mixed-stage worm lysate fractions were loaded and resolved on precast 4-15% gradient SDS-PAGE gels and transferred to PVDF membrane as recommended by the manufacturer (Bio-Rad). On immunoblots, human TDP-43 was detected with a commercially available monoclonal antibody ab57105 (Abcam) directed against human TDP-43 amino acids 1-261. TDP-43 phosphorylated at S409/S410 was detected by a monoclonal antibody called anti phospho TDP-43 (pS409/410) available from Cosmobio (catalog # TIP-PTD-M01). *C. elegans* β-tubulin levels were measured using monoclonal antibody E7 as a loading control as previously described [57, 58]. HRP labeled goat anti-mouse IgG was the secondary antibody (GE Healthcare) and used at a dilution of 1:4000. Dilutions were: 1:7500 for ab57105, 1:1000 for pS409/410, and 1:10000 for E7. Each immunoblot was repeated at least three times with independent experimental samples; representative blots are shown.

### Cell culture and siRNA

HEK 293 cells (from ATCC) were cultured under standard culture condition, Dulbecco's modified Eagle medium (DMEM), 10% defined fetal bovine serum (FBS), penicillin (50 IU/ml)–streptomycin (50 mg/ml). NSC-34 cells (Cedarlane Labs) were cultured in DMEM/HAM's F12 (50/50), 10% FBS, penicillin (50 IU/ml)–streptomycin (50 mg/ml). HEK 293 cells were treated with 150μM ethacrynic acid (EA) for 5 hours to induce endogenous TDP-43 phosphorylation [17]. NSC-34 cells were grown in differentiation medium (DMEM/HAM's F12 (50/50), 1% FBS, 1% non-essential amino acids (NEAA), penicillin (50 IU/ml)–streptomycin (50 mg/ml)) for one day prior to treatment with 50μM EA for 5 hours. RNAi experiments were carried out as per protocol in the TriFECTa Dicer-Substrate RNAi manual (Integrated DNA Technologies). For inhibitor assays, cells were treated with the indicated concentration of PHA767491 (Tocris Bioscience) or DMSO (vehicle) 2 hours prior to induction of TDP-43 phosphorylation with EA.

### Kinase assays

GST-TDP-43 (WT) and GST-TDP-43 (M337V) fusion proteins were purified from BL21(DE3) expression host cells as previously described [59]. Active kinase enzymes were obtained commercially via purification from HEK 293 cells—CDC7 and TTBK2 (Signalchem) and TTBK1 (Origene). Enzyme assays were carried out according to the manufacturer's instructions (Signalchem) in a kinase reaction buffer containing 25 mM MOPS, 12.25 mM glycerol-phosphate, 25 mM MgCl, 5 mM EGTA, 2 mM EDTA, 0.25 mM DTT and 50 μM ATP.

### Viability analysis

Parent worms homozygous for wCDC7 o/ex transgene (PFw25B3.3::*cdc-7*) but heterozygous for the other transgene of interest were generated by performing a standard mating cross of the two strains, and scoring F2 progeny (F3 animals) for the desired genotype. F3 animals were singled blind with regards to transgene status onto individual plates with food, and their progeny scored for the transgene of interest. Percent lethality was calculated based on the expected Mendelian ratios of progeny for one segregating trait (expect 25% homozygous ++, 50% heterozygous +−, and 25% homozygous −−).

### Neurodegeneration assays

A synchronized population of animals was obtained following timed egg lays at 25°C and scored at the indicated developmental stages. Live worms were placed on a 3% agarose pad containing 0.01% sodium azide to immobilize the worms. Worms were imaged under fluorescence microscopy and scored for number of GABAergic neurons. Data were analyzed using GraphPad Prism software. Fluorescent and Differential Interference Contrast (DIC) microscopy was performed on a DeltaVision Elite imaging system. Image acquisition and deconvolution was performed with SoftWorx 5.0. Image processing with Adobe Photoshop consisted of adjustments of brightness and contrast to optimize visualization.

### Inhibitor assays

Drug plates were prepared by spreading the desired concentration of inhibitor evenly across the surface of a standard NGM *C. elegans* culture plate and drug was allowed to diffuse throughout the plate for 18 hours. Strains used in inhibitor assays included the cuticle defective *bus-8(e1368)* mutation to enhance drug entry into the animals[60]. A synchronized population was obtained following timed egg lays at 20°C, and effects on behavior, growth, and neuronal integrity were recorded at day 1 of adulthood.

### Human Tissue and Immunohistochemistry

Post-mortem brain tissue was obtained from the University of Washington Alzheimer's Disease Research Center (Seattle, WA), where permission for use of tissue in scientific experiments was obtained. FTLD cases were selected on the basis of having a clinical or autopsy-confirmed diagnosis of FTLD and FTLD-related disorders. One case was identified with a mutation in progranulin. Control samples were from neurologically healthy control participants, who were of a similar age. Primary antibodies used for immunohistochemistry were anti-CDC7 (clone DCS-342, MBL, 1:100) and anti-phospho TDP-43 409/410 (CosmoBio, 1:1000). Additional details in Supplementary Methods. For double labeling experiments, sections were first immunostained with anti-phospho TDP-43 and reaction product was visualized with nickel enhanced DAB (black). Sections were then immunostained with anti-CDC7 and visualized with DAB alone (brown).

## Supplementary Material

Refer to Web version on PubMed Central for supplementary material.

## Acknowledgments

We thank the reviewers and editors for helpful comments and suggestions. This work was supported by grants from the Department of Veterans Affairs [Merit Review Grant #1147891 to B.K. and Career Development Award (CDA1) to N.L.], NIA training grant [AG 000057-31 to N.L.], and National Institutes of Health [R01NS064131 to B.K., 2P50AG005136-27 and 5P50NS2062684-02 to J.L.]). We thank the National Bioresource Project (Japan) and *C. elegans* Genetics Center for providing strains. We thank Elaine Loomis, Lynne Greenup, Aleen Saxton, and Tobin Martin for outstanding technical assistance, and Jeanna Wheeler for assisting in the design of the neuronal RNAi transgene constructs. We thank Andrew Fire for *C. elegans* expression plasmids, Yishi Jin for strain CZ1200, James Rand for plasmid RM#509p, and the Developmental Studies Hybridoma Bank (NICHD) for the β-tubulin antibody E7. We thank Julie Ahringer and Mark Vidal for production of RNAi libraries from which the kinase targeting clones were retrieved.

## REFERNCES

1. Zhang J, Yang PL, Gray NS. Targeting cancer with small molecule kinase inhibitors. Nat Rev Cancer. Jan; 2009 9(1):28–39. [PubMed: 19104514]
2. Chico LK, Van Eldik LJ, Watterson DM. Targeting protein kinases in central nervous system disorders. Nat Rev Drug Discov. Nov; 2009 8(11):892–909. [PubMed: 19876042]
3. Neumann M, Sampathu DM, Kwong LK, et al. Ubiquitinated TDP-43 in frontotemporal lobar degeneration and amyotrophic lateral sclerosis. Science. Oct 6; 2006 314(5796):130–3. [PubMed: 17023659]
4. Arai T, Hasegawa M, Akiyama H, et al. TDP-43 is a component of ubiquitin-positive tau-negative inclusions in frontotemporal lobar degeneration and amyotrophic lateral sclerosis. Biochem Biophys Res Commun. Dec 22; 2006 351(3):602–11. [PubMed: 17084815]
5. Chen-Plotkin AS, Lee VM, Trojanowski JQ. TAR DNA-binding protein 43 in neurodegenerative disease. Nat Rev Neurol. Apr; 2010 6(4):211–20. [PubMed: 20234357]
6. Wijesekera LC, Leigh PN. Amyotrophic lateral sclerosis. Orphanet J Rare Dis. 2009; 4:3. [PubMed: 19192301]
7. Cardarelli R, Kertesz A, Knebl JA. Frontotemporal dementia: a review for primary care physicians. Am Fam Physician. Dec; 2010 82(11):1372–7. [PubMed: 21121521]
8. DeJesus-Hernandez M, Mackenzie IR, Boeve BF, et al. Expanded GGGGCC hexanucleotide repeat in noncoding region of C9ORF72 causes chromosome 9p-linked FTD and ALS. Neuron. Oct; 2011 72(2):245–56. [PubMed: 21944778]
9. Renton AE, Majounie E, Waite A, et al. A hexanucleotide repeat expansion in C9ORF72 is the cause of chromosome 9p21-linked ALS-FTD. Neuron. Oct; 2011 72(2):257–68. [PubMed: 21944779]

10. Hasegawa M, Nonaka T, Tsuji H, et al. Molecular dissection of TDP-43 proteinopathies. J Mol Neurosci. Nov; 2011 45(3):480–5. [PubMed: 21678031]
11. Nelson PT, Schmitt FA, Lin Y, et al. Hippocampal sclerosis in advanced age: clinical and pathological features. Brain. May; 2011 134(Pt 5):1506–18. [PubMed: 21596774]
12. Hasegawa M, Arai T, Nonaka T, et al. Phosphorylated TDP-43 in frontotemporal lobar degeneration and amyotrophic lateral sclerosis. Ann Neurol. Jun 10.2008
13. Neumann M, Kwong LK, Lee EB, et al. Phosphorylation of S409/410 of TDP-43 is a consistent feature in all sporadic and familial forms of TDP-43 proteinopathies. Acta Neuropathol. Jan 6.2009
14. Inukai Y, Nonaka T, Arai T, et al. Abnormal phosphorylation of Ser409/410 of TDP-43 in FTLD-U and ALS. FEBS Lett. Aug 20; 2008 582(19):2899–904. [PubMed: 18656473]
15. Liachko NF, Guthrie CR, Kraemer BC. Phosphorylation Promotes Neurotoxicity in a Caenorhabditis elegans Model of TDP-43 Proteinopathy. J Neurosci. Dec 1; 2010 30(48):16208–19. [PubMed: 21123567]
16. Kametani F, Nonaka T, Suzuki T, et al. Identification of casein kinase-1 phosphorylation sites on TDP-43. Biochem Biophys Res Commun. May 1; 2009 382(2):405–9. [PubMed: 19285963]
17. Iguchi Y, Katsuno M, Takagi S, et al. Oxidative stress induced by glutathione depletion reproduces pathological modifications of TDP-43 linked to TDP-43 proteinopathies. Neurobiol Dis. Mar; 2012 45(3):862–70. [PubMed: 22198567]
18. Tomizawa K, Omori A, Ohtake A, Sato K, Takahashi M. Tau-tubulin kinase phosphorylates tau at Ser-208 and Ser-210, sites found in paired helical filament-tau. Febs Letters. Mar 16; 2001 492(3): 221–7. 2001. [PubMed: 11257498]
19. Sato S, Cerny RL, Buescher JL, Ikezu T. Tau-tubulin kinase 1 (TTBK1), a neuron-specific tau kinase candidate, is involved in tau phosphorylation and aggregation. J Neurochem. Sep; 2006 98(5):1573–84. [PubMed: 16923168]
20. Vázquez-Higuera JL, Mateo I, Sánchez-Juan P, et al. Genetic variation in the tau kinases pathway may modify the risk and age at onset of Alzheimer's disease. J Alzheimers Dis. 2011; 27(2):291–7. [PubMed: 21811019]
21. Yu NN, Yu JT, Xiao JT, et al. Tau-tubulin kinase-1 gene variants are associated with Alzheimer's disease in Han Chinese. Neurosci Lett. Mar; 2011 491(1):83–6. [PubMed: 21219968]
22. Houlden H, Johnson J, Gardner-Thorpe C, et al. Mutations in TTBK2, encoding a kinase implicated in tau phosphorylation, segregate with spinocerebellar ataxia type 11. Nat Genet. Dec; 2007 39(12):1434–6. [PubMed: 18037885]
23. Shaye DD, Greenwald I. OrthoList: a compendium of C. elegans genes with human orthologs. PLoS One. 2011; 6(5):e20085. [PubMed: 21647448]
24. Bousset K, Diffley JF. The Cdc7 protein kinase is required for origin firing during S phase. Genes Dev. Feb; 1998 12(4):480–90. [PubMed: 9472017]
25. Takahashi TS, Basu A, Bermudez V, Hurwitz J, Walter JC. Cdc7-Drf1 kinase links chromosome cohesion to the initiation of DNA replication in Xenopus egg extracts. Genes Dev. Jul; 2008 22(14):1894–905. [PubMed: 18628396]
26. Matos J, Lipp JJ, Bogdanova A, et al. Dbf4-dependent CDC7 kinase links DNA replication to the segregation of homologous chromosomes in meiosis I. Cell. Nov; 2008 135(4):662–78. [PubMed: 19013276]
27. Costanzo V, Shechter D, Lupardus PJ, Cimprich KA, Gottesman M, Gautier J. An ATR- and Cdc7-dependent DNA damage checkpoint that inhibits initiation of DNA replication. Mol Cell. Jan; 2003 11(1):203–13. [PubMed: 12535533]
28. Baker M, Mackenzie IR, Pickering-Brown SM, et al. Mutations in progranulin cause tau-negative frontotemporal dementia linked to chromosome 17. Nature. Aug 24; 2006 442(7105):916–9. [PubMed: 16862116]
29. Cruts M, Gijselinck I, van der Zee J, et al. Null mutations in progranulin cause ubiquitin-positive frontotemporal dementia linked to chromosome 17q21. Nature. Aug 24; 2006 442(7105):920–4. [PubMed: 16862115]

30. Montagnoli A, Valsasina B, Croci V, et al. A Cdc7 kinase inhibitor restricts initiation of DNA replication and has antitumor activity. Nat Chem Biol. Jun; 2008 4(6):357–65. [PubMed: 18469809]

31. Vanotti E, Amici R, Bargiotti A, et al. Cdc7 kinase inhibitors: pyrrolopyridinones as potential antitumor agents. 1. Synthesis and structure-activity relationships. J Med Chem. Feb; 2008 51(3): 487–501. [PubMed: 18201066]

32. Fraser AG, Kamath RS, Zipperlen P, Martinez-Campos M, Sohrmann M, Ahringer J. Functional genomic analysis of C. elegans chromosome I by systematic RNA interference. Nature. Nov 16; 2000 408(6810):325–30. 2000. [PubMed: 11099033]

33. Lee J, Nam S, Hwang SB, et al. Functional genomic approaches using the nematode Caenorhabditis elegans as a model system. J Biochem Mol Biol. Jan; 2004 37(1):107–13. [PubMed: 14761308]

34. Kraemer BC, Burgess JK, Chen JH, Thomas JH, Schellenberg GD. Molecular pathways that influence human tau-induced pathology in Caenorhabditis elegans. Hum Mol Genet. May 1; 2006 15(9):1483–96. [PubMed: 16600994]

35. Hamamichi S, Rivas RN, Knight AL, Cao S, Caldwell KA, Caldwell GA. Hypothesis-based RNAi screening identifies neuroprotective genes in a Parkinson's disease model. Proc Natl Acad Sci U S A. Jan; 2008 105(2):728–33. [PubMed: 18182484]

36. Kuwahara T, Koyama A, Koyama S, et al. A systematic RNAi screen reveals involvement of endocytic pathway in neuronal dysfunction in alpha-synuclein transgenic C. elegans. Hum Mol Genet. Oct 1; 2008 17(19):2997–3009. [PubMed: 18617532]

37. Kim BJ, Kim SY, Lee H. Identification and characterization of human cdc7 nuclear retention and export sequences in the context of chromatin binding. J Biol Chem. Oct; 2007 282(41):30029–38. [PubMed: 17711849]

38. Sato N, Sato M, Nakayama M, Saitoh R, Arai K, Masai H. Cell cycle regulation of chromatin binding and nuclear localization of human Cdc7-ASK kinase complex. Genes Cells. May; 2003 8(5):451–63. [PubMed: 12694534]

39. Kim JM, Yamada M, Masai H. Functions of mammalian Cdc7 kinase in initiation/monitoring of DNA replication and development. Mutat Res. Nov; 2003 532(1-2):29–40. [PubMed: 14643427]

40. Oshiro G, Owens JC, Shellman Y, Sclafani RA, Li JJ. Cell cycle control of Cdc7p kinase activity through regulation of Dbf4p stability. Mol Cell Biol. Jul; 1999 19(7):4888–96. [PubMed: 10373538]

41. Weinreich M, Stillman B. Cdc7p-Dbf4p kinase binds to chromatin during S phase and is regulated by both the APC and the RAD53 checkpoint pathway. EMBO J. Oct; 1999 18(19):5334–46. [PubMed: 10508166]

42. Ferreira MF, Santocanale C, Drury LS, Diffley JF. Dbf4p, an essential S phase-promoting factor, is targeted for degradation by the anaphase-promoting complex. Mol Cell Biol. Jan; 2000 20(1):242–8. [PubMed: 10594027]

43. Ayala YM, Zago P, D'Ambrogio A, et al. Structural determinants of the cellular localization and shuttling of TDP-43. J Cell Sci. Nov 15; 2008 121(Pt 22):3778–85. [PubMed: 18957508]

44. Zhang YJ, Gendron TF, Xu YF, Ko LW, Yen SH, Petrucelli L. Phosphorylation regulates proteasomal-mediated degradation and solubility of TAR DNA binding protein-43 C-terminal fragments. Mol Neurodegener. 2010; 5:33. [PubMed: 20804554]

45. Brady OA, Meng P, Zheng Y, Mao Y, Hu F. Regulation of TDP-43 aggregation by phosphorylation and p62/SQSTM1. J Neurochem. Jan; 2011 116(2):248–59. [PubMed: 21062285]

46. Kabashi E, Lin L, Tradewell ML, et al. Gain and loss of function of ALS-related mutations of TARDBP (TDP-43) cause motor deficits in vivo. Hum Mol Genet. Feb 15; 2010 19(4):671–83. [PubMed: 19959528]

47. Zhao C, Tovar C, Yin X, et al. Synthesis and evaluation of pyrido-thieno-pyrimidines as potent and selective Cdc7 kinase inhibitors. Bioorg Med Chem Lett. Jan; 2009 19(2):319–23. [PubMed: 19071019]

48. Koltun ES, Tsuhako AL, Brown DS, et al. Discovery of XL413, a potent and selective CDC7 inhibitor. Bioorg Med Chem Lett. Jun; 2012 22(11):3727–31. [PubMed: 22560567]

49. Menichincheri M, Albanese C, Alli C, et al. Cdc7 kinase inhibitors: 5-heteroaryl-3-carboxamido-2-aryl pyrroles as potential antitumor agents. 1. Lead finding. J Med Chem. Oct; 2010 53(20):7296–315. [PubMed: 20873740]
50. Menichincheri M, Bargiotti A, Berthelsen J, et al. First Cdc7 kinase inhibitors: pyrrolopyridinones as potent and orally active antitumor agents. 2. Lead discovery. J Med Chem. Jan; 2009 52(2): 293–307. [PubMed: 19115845]
51. Shafer CM, Lindvall M, Bellamacina C, et al. 1H-indazol-5-yl)-6-phenylpyrimidin-2(1H)-one analogs as potent CDC7 inhibitors. Bioorg Med Chem Lett. Aug; 2008 18(16):4482–5. [PubMed: 18672368]
52. Huang C, Tong J, Bi F, Zhou H, Xia XG. Mutant TDP-43 in motor neurons promotes the onset and progression of ALS in rats. J Clin Invest. Jan; 2012 122(1):107–18. [PubMed: 22156203]
53. Plowman GD, Sudarsanam S, Bingham J, Whyte D, Hunter T. The protein kinases of Caenorhabditis elegans: a model for signal transduction in multicellular organisms. Proc Natl Acad Sci U S A. Nov; 1999 96(24):13603–10. [PubMed: 10570119]
54. Kamath RS, Fraser AG, Dong Y, et al. Systematic functional analysis of the Caenorhabditis elegans genome using RNAi. Nature. 2003; 2003:421–231.
55. Rual JF, Ceron J, Koreth J, et al. Toward improving Caenorhabditis elegans phenome mapping with an ORFeome-based RNAi library. Genome Res. Oct; 2004 14(10B):2162–8. [PubMed: 15489339]
56. Wang D, Kennedy S, Conte D, et al. Somatic misexpression of germline P granules and enhanced RNA interference in retinoblastoma pathway mutants. Nature. Jul; 2005 436(7050):593–7. [PubMed: 16049496]
57. Kraemer BC, Schellenberg GD. SUT-1 enables tau-induced neurotoxicity in C. elegans. Hum Mol Genet. Aug 15; 2007 16(16):1959–71. [PubMed: 17576746]
58. Guthrie CR, Schellenberg GD, Kraemer BC. SUT-2 potentiates tau-induced neurotoxicity in Caenorhabditis elegans. Hum Mol Genet. May 15; 2009 18(10):1825–38. [PubMed: 19273536]
59. Buratti E, Brindisi A, Giombi M, Tisminetzky S, Ayala YM, Baralle FE. TDP-43 binds heterogeneous nuclear ribonucleoprotein A/B through its C-terminal tail: an important region for the inhibition of cystic fibrosis transmembrane conductance regulator exon 9 splicing. J Biol Chem. Nov 11; 2005 280(45):37572–84. [PubMed: 16157593]
60. Partridge FA, Tearle AW, Gravato-Nobre MJ, Schafer WR, Hodgkin J. The C. elegans glycosyltransferase BUS-8 has two distinct and essential roles in epidermal morphogenesis. Dev Biol. May 15; 2008 317(2):549–59. [PubMed: 18395708]

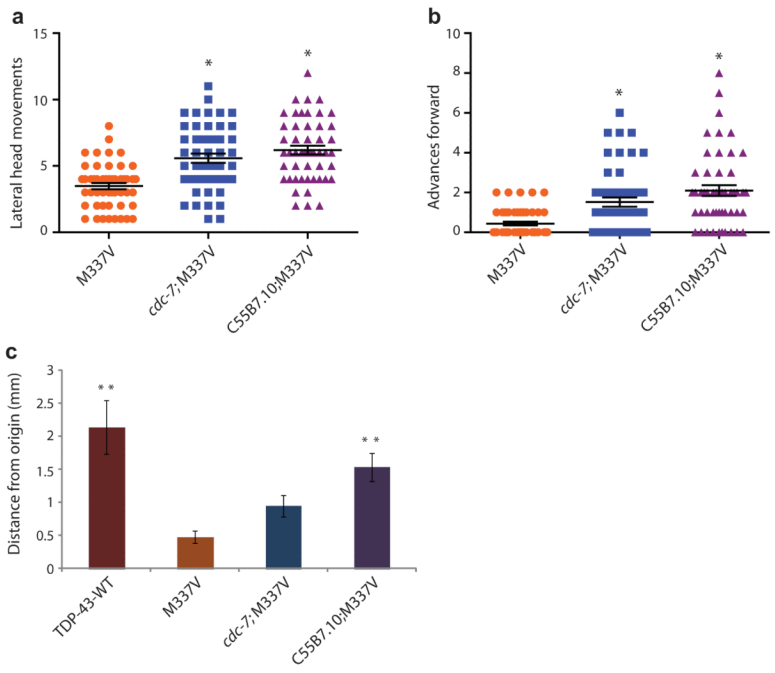


**Figure 1. Kinase mutants *cdc-7*(−/−) and C55B7.10 (−/−) improve the movement defects of TDP-43 transgenic animals**

**(a)** Stage synchronized day 1 adult *cdc-7*(−/−) and C55B7.10(−/−) kinase mutants have significantly more head movements to the left or right of the central body axis than TDP-43 M337V transgenic animals alone. All animals for movement assays were grown at 25°C. N=50 for each genotype. **P* <0.05 versus M337V. Statistical significance was determined using one-way ANOVA with Tukey's multiple-comparison test. **(b)** Kinase mutant animals move forward significantly more times than M337V transgenic animals alone. **(c)** Stage synchronized L4 kinase mutant animals move significantly greater distances than M337V transgenic animals alone, comparable to the distances traveled by wild-type TDP-43 (TDP-43-WT) transgenic animals. N>50 for each genotype. ***P* <0.05 versus M337V. See also Figure S1.

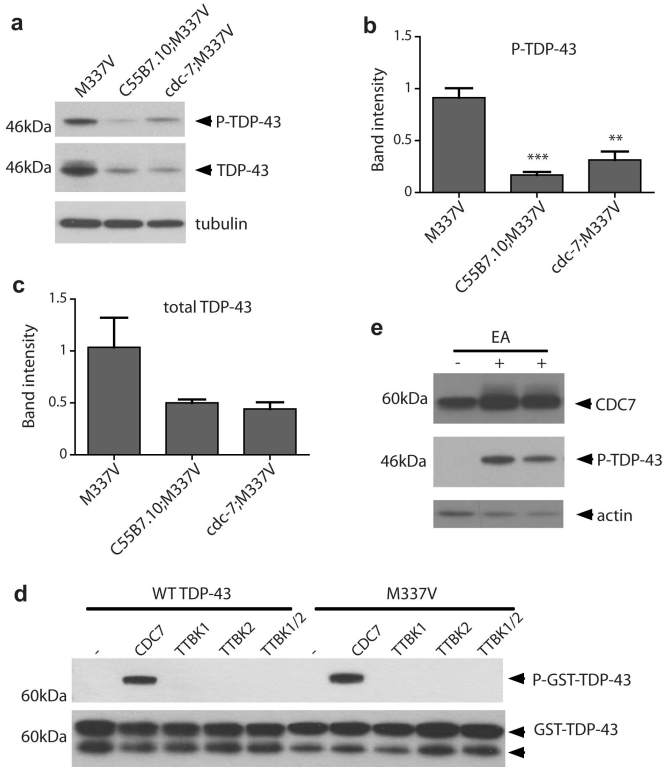


**Figure 2. *cdc-7* and C55B7.10 phosphorylate TDP-43 in *C. elegans***

**(a)** *cdc-7*(−/−);M337V and C55B7.10(−/−);M337V transgenic animals have reduced phosphorylated S409/410 TDP-43 compared to M337V alone. Mixed populations of animals were grown for analysis. **(b)** The average intensity of the immunoreactive immunoblot bands are determined for three independent replicate Western blots comparing phosphorylated S409/410 TDP-43 in M337V, C55B7.10(-);M337V, and *cdc-7(-)*;M337V animals. ***$P$ <0.001 versus M337V. **$P$ <0.01 versus M337V. Statistical significance was determined using one-way ANOVA with Tukey's multiple-comparison test. **(c)** The average intensity of the immunoreactive immunoblot bands are determined for three independent replicate Western blots comparing total TDP-43 in M337V, C55B7.10(-);M337V, and *cdc-7(-)*;M337V animals. Differences between strains are not statistically significant. $P$ >0.05. **(d)** Purified CDC7 phosphorylates wild-type (WT) and mutant M337V (337) GST-tagged TDP-43 *in vitro*, while TTBK1 or TTBK2 did not phosphorylate TDP-43 either singly or when combined in one reaction. **(e)** Glutathione depletion with 150μM ethacrynic acid increases levels of CDC7 and phosphorylated TDP-43 in HEK 293 cells.

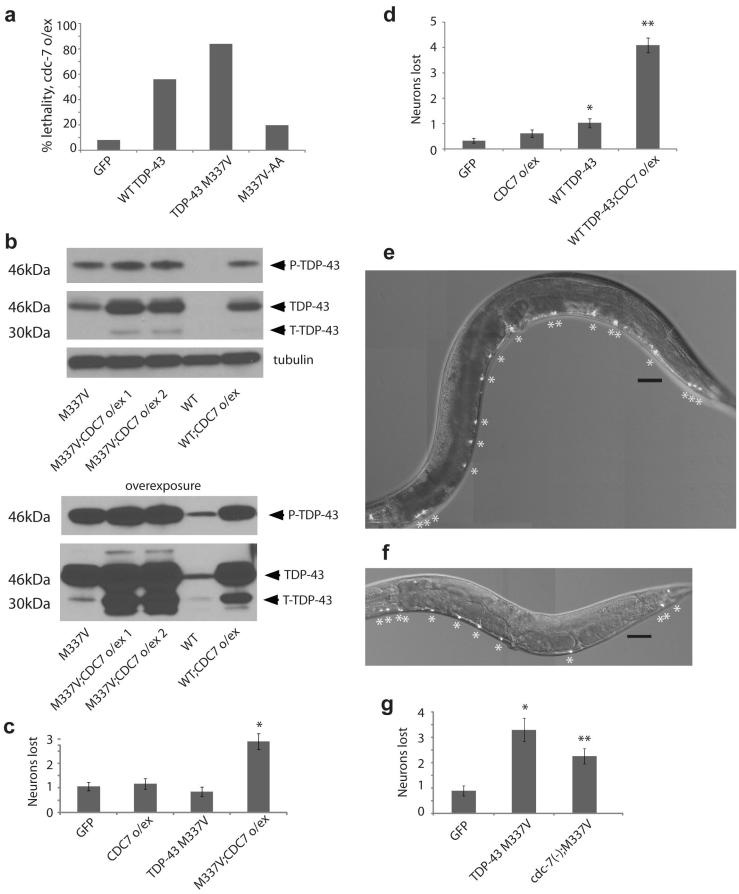


**Figure 3. *cdc-7* o/ex promotes TDP-43 toxicity in *C. elegans***

**(a)** Overexpression of *cdc-7* is synthetic lethal with mutant TDP-43. Percentage lethality observed of the double homozygote transgenic animals with *cdc-7* o/ex and either GFP (8%), wild type TDP-43 (56%), mutant M337V (84%), or non-phosphorylatable M337V S409/410A (20%) animals. N>180 for all genotypes tested. See also Supplementary Table 3. **(b)** Overexpression of wCDC7 drives increased levels of total, phosphorylated and truncated TDP-43 in *C. elegans*. The same immunoblot is shown at two different exposures to allow visualization of WT TDP-43 levels. **(c)** M337V;*cdc-7* o/ex animals have significant neuronal loss compared to GABA::GFP, *cdc-7* o/ex, and M337V animals at larval stage L4. Animals were grown at 25°C. N>30 animals. **P* <0.0001, ANOVA with Tukey's multiple-comparison test. **(d)** WT TDP-43;*cdc-7* o/ex animals have significant neuronal loss compared to GABA::GFP, *cdc-7* o/ex, and WT TDP-43 alone at day 2 of adulthood N>30 animals. ** *P* <0.0001. WT TDP-43 has significant neuronal loss relative to GABA::GFP alone. **P* <0.002. **(e)** A representative WT TDP-43 animal does not have significant neurodegeneration at day 2 of adulthood. Worm head is left, and 18 neuron cell bodies along the ventral nerve cord are visualized with GABA::GFP fluorescence and marked with asterisks. Scale bar represents 40μm. **(f)** WT-TDP-43;*cdc-7* o/ex animals have significant neuronal loss at day 2 of adulthood and smaller body size relative to WT-TDP-43 animals. 12 neuron cell bodies are marked with asterisks. **(g)** TDP-43 M337V animals have significant neuronal loss relative to GFP alone at day 1 of adulthood. *cdc-7*(−/−);M337V animals have significantly less neuronal loss than TDP-43 M337V; n=30; *P*<0.0001.

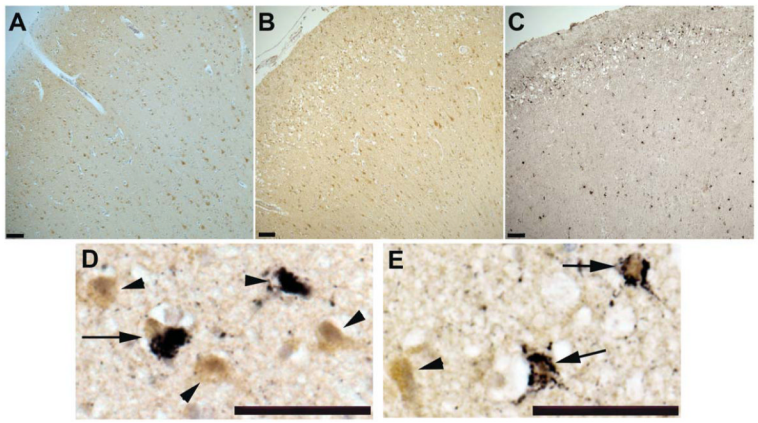


**Figure 4. CDC7 and phosphorylated TDP-43 are co-expressed in frontal cortex neurons of FTLD cases**

**(a)** Representative photomicrographs demonstrating CDC7 immunoreactivity in the cytoplasm of cortical neurons in normal frontal cortex. Immunoreactive neurons in deeper layers are more prevalent. **(b)** FTLD cases display similar CDC7 immunoreactivity to controls. **(c)** Phospho TDP-43 immunoreactivity in cortical layer 2 as well as deeper layers in an FTLD case. **(d,e)** Representative images demonstrating double labeling of CDC7 (brown) and phosphorylated TDP-43 (black) in an FTLD case. Arrows show cells double labeled with both proteins. Arrowheads show cells labeled with only CDC7 or phospho TDP-43. Scale bars: 100μm, A-C and 50μm D, E.

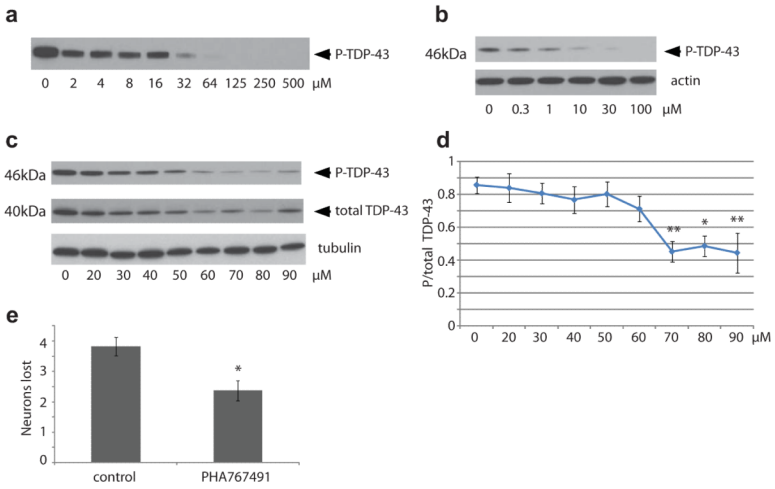


**Figure 5. Small molecule inhibition of CDC7 by PHA767491 prevents TDP-43 phosphorylation and neurodegeneration**

**(a)** PHA767491 prevents phosphorylation of purified M337V mutant TDP-43 *in vitro*. **(b)** Increasing concentrations of PHA767491 prevents pathological phosphorylation of endogenous TDP-43 in differentiated motor neuron-like NSC-34 cells treated with 50μM ethacrynic acid. **(c)** Mixed populations of transgenic *C. elegans* grown at 20°C in the presence of PHA767491 have significantly reduced TDP-43 phosphorylation with increasing concentrations of inhibitor (see panel **d**). Total TDP-43 levels are also apparently reduced, but this reduction is not significantly different than control treatments upon band quantitation and statistical analysis of multiple independent experiments (data not shown, $P$ >0.05 by one-way ANOVA with Dunnett's Multiple Comparison Test). **(d)** Graph of phosphorylated TDP-43 relative to total TDP-43 at each concentration of inhibitor in PHA767491 treated *C. elegans* (panel **c**). Relative band intensities are graphed in arbitrary units. The average intensities are determined for four independent replicate Western blots of total and phosphorylated TDP-43. ** $P$ <0.01, * $P$ <0.05 versus vehicle control (0μM PHA76749). Statistical significance was determined using one-way ANOVA with Dunnett's Multiple Comparison Test. **(e)** M337V TDP-43 transgenic *C. elegans* grown in the presence of 70 μM PHA767491 lose significantly fewer GABAergic motor neurons than animals grown in the presence of DMSO alone. Animals were raised at 20°C. Scoring was performed at day 1 of adulthood. * $P$ =0.0007, unpaired two-tailed t test, N>26.

## Table 1
## Candidate TDP-43 kinases identified by RNAi screening

| *C. elegans* Gene[a] | Human Homolog[b] | Kinase Family[c] | Group[c] | # ID'd/# in Kinome[d] | Putative Function[e] | Mutant[f] | Phos.[g] | Movement[h] |
|---|---|---|---|---|---|---|---|---|
| *pkc-1* | PRKCH | PKC | AGC | (1/1) | Modulates ERK and JNK signaling; associated with infarct, arthritis, and gastric atrophy | nj4 | − | − |
| *zyg-8* | DCLK1 | DCAM-KL | CAMK | (1/1) | Regulates microtubule polymerization; associated with memory and cognitive function | b235 | − | − |
| C55B7.10 | TTBK1/2 | Worm6 | CK1 | (2/28) | Phosphorylates tau; mutation of TTBK2 causes spinocerebellar ataxia type 11; TTBK1 associated with Alzheimer's disease | tm4189 | ++ | ++ |
| T09B4.7 | TTBK1/2 | Worm6 | CK1 | (2/28) | | tm4127 | − | − |
| C05C12.1 | TTBK1/2 | TTBKL | CK1 | (2/34) | | tm3851 | − | − |
| C49C3.10 | MAPK9 | MAPK | CMGC | (1/5) | Involved in cell proliferation, apoptosis, transcription factor activation | tm3933 | − | − |
| C01H6.9 | GSG2 | Haspin | Other | (2/13) | Phosphorylates histone H3; important for mitotic chromosome cohesion | tm3858 * | NA | − |
| ZK177.2 | GSG2 | Haspin | Other | (2/13) | | tm4845 | − | − |
| *cdc-7* | CDC7 | CDC7 | Other | (1/1) | Regulates S-phase and chromatin assembly, acts in DNA replication and damage response | tm4391 | ++ | ++ |
| *gcy-17* | NPR1 | RGC | RGC | (2/27) | Guanylate cyclase that regulates blood pressure; associated with hypertension and cardiovascular disease | tm4516 | − | − |
| *gcy-27* | GUCY2D | RGC | RGC | (2/27) | Membrane guanylate cyclase associated with Lerber congenital amaurosis type 1 | ok3653 | − | − |
| *mlk-1* | MAP3K9 | MLK | TKL | (1/2) | Activates JNK signaling cascade; important for axonal regeneration and neuronal apoptosis | ok2471 | − | − |

[a] Kinase suppressors of TDP-43 movement defects, identified by RNAi.

[b] The human homologs of *C. elegans* genes are the best candidates identified by BLAST protein analysis (HUGO gene nomenclature).

[c] *C. elegans* kinases are assigned to a kinase family and group based on protein sequence analysis (Manning, 2005). See also Table S1.

[d] The number of kinase family members identified as TDP-43 suppressors is compared to the total number of kinases within that family.

[e] Some of the known functions of the human kinase genes are highlighted.

[f] Deletion mutant alleles available for *C. elegans* kinases.

* lethal; candidate was screened using constitutive neuronal RNAi targeting C01H6.9.

[g]Kinase mutants were tested for changes in TDP-43 phosphorylation by immunblotImmunoblot. Mutants with visible decreases in TDP-43 phosphorylation are marked with ++. NA: not tested.

[h]Kinase mutants were tested for changes in TDP-43-dependent movement defects by radial locomotion. Mutants with significantly improved movement are marked with ++.